# VALIDATION OF GAUSSIAN SELF-FIELD MODELS FOR SPACE-CHARGE DOMINATED INJECTORS

O. Betteridge*[1,3], R. J. Apsimon[2,3], and Ö. Apsimon[1,3]
[1]Department of Physics and Astronomy, The University of Manchester, Manchester, United Kingdom
[2]Department of Engineering, Lancaster University, Lancaster, United Kingdom
[3]Cockcroft Institute of Accelerator Science and Technology, Daresbury, United Kingdom

*Abstract*

We benchmark analytic and numerical self-field models for a near-Gaussian photoinjector bunch. Kim's analytic three-dimensional Gaussian model is compared with OPAL's mesh-based space-charge solver and two in-house calculations: direct Coulomb summation and FFT-based Green-function convolution. The comparison is performed in the bunch rest frame for a 100 pC, $\gamma \approx 12$ Gaussian bunch. The transverse electric fields show strong agreement between Kim's model and OPAL, supporting the use of the analytic model as a fast benchmark for near-Gaussian bunches. The longitudinal field is more sensitive to bunch asymmetry and boundary treatment, revealing small systematic differences between methods. These results clarify the practical limits of Gaussian analytic models and provide a controlled validation case for numerical space charge solvers.

## INTRODUCTION

Space charge is a dominant source of emittance growth in low-energy, high-brightness photoinjectors [1–4]. At the injector exit, the bunch is still only moderately relativistic, so the internal Coulomb field can strongly affect the transverse phase space. Reliable self-field modelling is therefore needed both for designing emittance-compensation schemes and for interpreting particle-tracking simulations.

Analytic models are useful because they provide fast checks on the size, scaling, and symmetry of the self-fields. They are especially valuable when testing numerical solvers, where mesh resolution, interpolation, boundary conditions, and finite-particle noise can all influence the calculated field [5–7]. However, analytic models usually assume an idealised charge distribution. In photoinjectors this assumption is only approximate: the bunch may develop non-Gaussian tails, transverse asymmetry, longitudinal skew, or correlations introduced by the cathode laser, RF curvature, and space-charge evolution. These effects limit the range over which an analytic Gaussian model can be expected to agree with a full particle-based calculation.

The purpose of this paper is to use a deliberately simple test case to compare analytic and numerical self-field calculations. Kim's analytic three-dimensional Gaussian model [8] is used as a reference and is compared with OPAL's mesh-based space-charge solver, a direct particle-particle Coulomb calculation, and an in-house FFT-based Green-function convolution. The comparison is made in the bunch rest frame for a single bunch. This isolates the self-field calculation itself, rather than the full injector dynamics, and allows differences between the methods to be identified more clearly.

* oliver.betteridge@postgrad.manchester.ac.uk

## SPACE CHARGE MODELS

Kim's model gives analytic expressions for the electric field of a three-dimensional Gaussian bunch [8]. In this work the bunch is treated as cylindrically symmetric, with rms transverse size $\sigma_r$, rms longitudinal size $\sigma_z$, and aspect ratio

$$A = \frac{\sigma_r}{\sigma_z}. \tag{1}$$

All coordinates are referenced to the bunch centre, with $r^2 = x^2 + y^2$. The normalised transverse and longitudinal field functions used in the comparison are

$$\Lambda_x(r,z) = \frac{r}{\sigma_r^2}\int_0^\infty \frac{\exp\left[-\frac{1}{2}\left(\frac{r^2}{\sigma_r^2(1+\zeta)} + \frac{z^2}{\sigma_z^2(1+A^2\zeta)}\right)\right]}{(1+\zeta)^2(1+A^2\zeta)^{1/2}}\,d\zeta, \tag{2}$$

and

$$\Lambda_z(r,z) = \frac{z}{\sigma_z^2}\int_0^\infty \frac{\exp\left[-\frac{1}{2}\left(\frac{r^2}{\sigma_r^2(1+\zeta)} + \frac{z^2}{\sigma_z^2(1+A^2\zeta)}\right)\right]}{(1+\zeta)^{3/2}(A^2+\zeta)}\,d\zeta. \tag{3}$$

Here $\Lambda_x$ and $\Lambda_z$ describe the normalised transverse and longitudinal self-fields, respectively. The corresponding space-charge electric-field components are obtained by applying the charge normalisation,

$$E_x^{\mathrm{SC}} = \frac{n_0}{4\pi\varepsilon_0}\Lambda_x, \qquad E_z^{\mathrm{SC}} = \frac{n_0}{4\pi\varepsilon_0}\Lambda_z, \tag{4}$$

to obtain the transverse and longitudinal contributions to the electric field, where $\varepsilon_0$ is the permittivity of free space and $n_0$ is the charge taken from the central bunch slice. The $x$ and $y$ components of the field are taken to be identical by cylindrical symmetry.

The OPAL comparison uses its standard mesh-based space charge treatment [9, 10]. Charged macroparticles are deposited onto a Cartesian mesh, the fields are solved on the grid, and the resulting electric fields are interpolated back to the particle positions using cloud-in-cell methods [5–7].

The direct Coulomb field is calculated as

$$\mathbf{E}_i = \frac{1}{4\pi\varepsilon_0}\sum_{j\neq i} q_j \frac{\mathbf{r}_i - \mathbf{r}_j}{\|\mathbf{r}_i - \mathbf{r}_j\|^3}, \tag{5}$$

which is computed by iterating through every particle and calculating its distance to every other particle in the bunch.

This method is computationally expensive and sensitive to shot noise. Shot noise arises from the discrete particle representation: in regions of high density, or when two particles are very close to each other, very large local electric fields can appear as localised spikes. This effect is particularly strong in the Coulomb method because it stems directly from the discrete nature of the calculation. Although the FFT method is also discrete, the charge is first deposited onto a mesh, allowing for a more uniform, continuous-like approximation of the field distribution.

The second in-house method computes the electric field as a convolution of the charge density with the free-space Green-function kernel,

$$E_\alpha(\mathbf{x}) = \mathcal{F}^{-1}\left\{\widehat{G_\alpha}(\mathbf{k})\,\widehat{\rho}(\mathbf{k})\right\}, \qquad \alpha \in \{x, y, z\}, \tag{6}$$

using three-dimensional FFTs. The charge is first deposited onto a mesh, so each grid cell contains the charge contribution from the nearby particles. This is different from OPAL, since cloud-in-cell assigns fractional charges to the mesh cells, i.e., treating the particles as clouds of charge, whereas here each particle's entire charge is assigned to the nearest cell. Since the FFT treats the mesh as repeating, the mesh is made larger than the bunch and the extra cells are set to zero charge (zero padding). This gives the field more empty space to decrease before it reaches the edge of the mesh. As a result, less field is artificially carried from one side of the mesh to the other, known as wrap-around effects, making the calculation closer to that of an isolated bunch in free space, which is the description of open boundary conditions.

## NUMERICAL SETUP

A Gaussian bunch with charge 100 pC and $\gamma \approx 12$ is used for all comparisons. The bunch is transformed into its rest frame before evaluating the fields, so that the comparison is made consistently with Kim's electrostatic model. The transformed coordinates are

$$x' = x - \langle x \rangle, \qquad y' = y - \langle y \rangle, \qquad z' = \gamma(z - \langle z \rangle), \tag{7}$$

with angle brackets denoting the average. The OPAL calculation uses a uniform Cartesian mesh. For the in-house FFT solver, the computational domain is padded by several beam sizes in each direction to reduce the aforementioned boundary wrap-around effects. The fields are compared through the central slice and the core of the bunch, where the particle density is highest and the differences between the models are easiest to see.

## FIELD COMPARISON

Figure 1 compares the total electric field in the central slice for all models. Kim's model and OPAL agree very well across the bunch, especially around the centre where the field drops towards zero and through the main rise on either side. This shows that, for this near-Gaussian case, OPAL is reproducing the same general field behaviour as the analytic model.

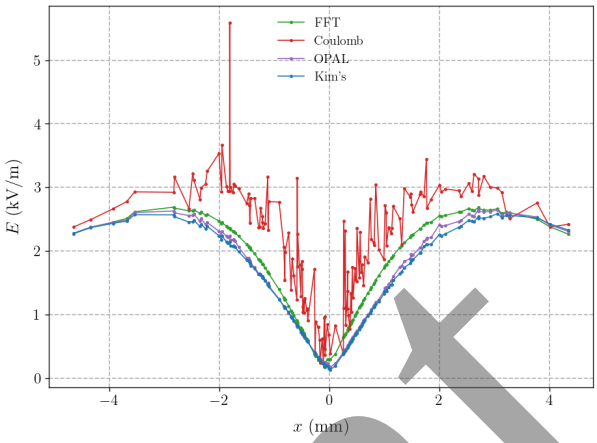


Figure 1: Total electric field in the central slice of a Gaussian bunch for the analytic, OPAL, direct Coulomb, and FFT-based models.

The FFT result follows the same overall shape, but rises slightly more sharply than those of OPAL and Kim's model and has a shifted minimum. This difference is likely due to the way the charge is deposited onto the mesh, finite grid resolution, and the zero padding used to approximate an isolated bunch. These effects change how sharply the field varies near the bunch core and tails.

The direct Coulomb calculation follows the broad trend, but contains strong local spikes. These are caused by nearest-neighbour particles in the distribution, which is the shot-noise effect discussed above. This shows why the direct Coulomb method is useful as a particle-level check, but not as a smooth field model on its own. Without some form of averaging or smoothing, the result is dominated by local particle noise.

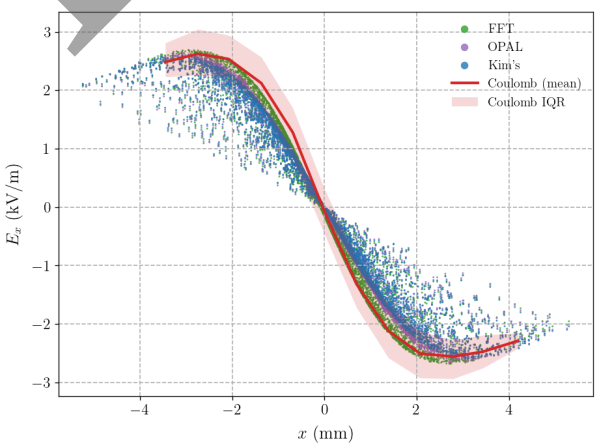


Figure 2: $x$-component of the transverse electric field in the central slice of the bunch.

Figure 2 shows the x-component of the transverse electric field in the same slice. The agreement between Kim's analytic model and OPAL is very good across the bunch core. The FFT model follows the same trend, with a small systematic overestimate that is, again, likely associated with

grid resolution, padding, and the treatment of the open boundary conditions. To remove the local shot noise from the Coulomb calculation, a moving-window average has been applied; the mean and interquartile range are plotted and are seen to be consistent with the other models.

The longitudinal field comparison is shown in Fig. 3. This component is more sensitive to the exact head-tail structure of the bunch, since Kim's model assumes a centred Gaussian distribution. It therefore predicts the zero crossing of $E_z$ at the bunch centre. The simulated bunch is not perfectly Gaussian longitudinally, with a slightly larger charge density towards the head of the bunch, which shifts the zero crossing and gives a larger field on that side. This explains why Kim's model underestimates the field towards the head: OPAL, the FFT calculation, and the direct Coulomb calculation all use the sampled particle distribution directly, while Kim's model only uses the rms beam sizes and assumes a symmetric Gaussian profile. Despite this, the overall longitudinal-field scale and shape remain consistent between the methods.

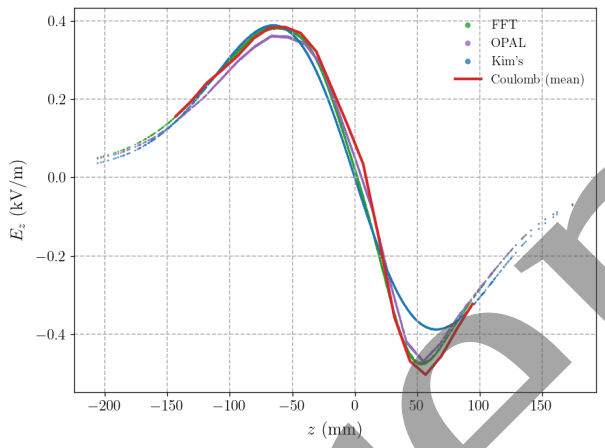


Figure 3: Longitudinal electric field through the bunch core.

The main result is that Kim's analytic model provides an accurate transverse-field benchmark for near-Gaussian bunches, while OPAL gives consistent self-fields in the regime tested here. When a distribution is strongly affected by space charge or other external fields, such as focusing elements and non-linear corrections, it can become distorted, weakening the approximations used by analytic models.

## CONCLUSION

Kim's analytic Gaussian self-field model, OPAL's mesh-based solver, and two in-house space-charge calculations have been compared for a 100 pC, $\gamma \approx 12$ near-Gaussian bunch in the bunch rest frame. The strongest agreement is found in the transverse field, where Kim's model and OPAL give consistent results for both the total field and the horizontal component $E_x$. This supports the use of the analytic model as a fast benchmark for near-Gaussian photoinjector bunches.

The direct Coulomb and FFT-convolution calculations reproduce the same general field trends, but also show the expected limitations of each method: local particle noise in the direct summation case and small mesh-related differences in the FFT case. The longitudinal field comparison is less exact, mainly because it is more sensitive to the actual head-tail structure of the sampled bunch than the transverse field.

Overall, the comparison shows that analytic Gaussian models are most useful as transverse-field benchmarks, while the longitudinal field provides a more sensitive test of distribution-level and numerical effects. This gives a controlled validation case for space-charge solvers used in low-energy photoinjector studies.

## ACKNOWLEDGEMENTS

The authors acknowledge the support of the Cockcroft Institute Core Grant, funded by UKRI under grant number UKRI1887.

## REFERENCES

[1] M. Reiser, "Linear beam optics with space charge: sections 4.1–4.4", in in *Theory and Design of Charged Particle Beams*, John Wiley & Sons, Ltd, 2008, chap. 4, pp. 163–232, ISBN: 9783527622047, doi:10.1002/9783527622047.ch4a,

[2] I. Hofmann, *Space charge physics for particle accelerators*. Cham, Switzerland: Springer, 2017. doi:10.1007/978-3-319-62157-9

[3] B. E. Carlsten, "Space-charge induced emittance compensation in high brightness photoinjectors", *Phys. Rev. E*, vol. 52, no. 5, pp. 5473–5480, 1995.

[4] L. Serafini, "Improving the beam quality of rf guns by correction of rf and space-charge effects", *AIP Conference Proceedings*, vol. 279, no. 1, pp. 645–674, 1992. doi:10.1063/1.44080

[5] R. W. Hockney and J. W. Eastwood, *Computer simulation using particles*. Boca Raton, FL: CRC Press, 1988. doi:10.1201/9780367806934

[6] C. K. Birdsall and A. B. Langdon, *Plasma physics via computer simulation*. Boca Raton, FL: CRC Press, 1991. doi:10.1201/9781315275048

[7] J. W. Eastwood, "Shaping the force law in two-dimensional particle–mesh models", *J. Comput. Phys.*, vol. 16, pp. 342–359, 1974. doi:10.1016/0021-9991(74)90044-8

[8] K.-J. Kim, "Rf and space-charge effects in laser-driven rf electron guns", *Nucl. Instrum. Methods Phys. Res., Sect. A*, vol. 275, no. 2, pp. 201–218, 1989. doi:10.1016/0168-9002(89)90688-8

[9] A. Adelmann *et al.*, "The opal framework", 2022, https://opalx-project.github.io/Manual/,

[10] J. Adelmann *et al.*, "Opal: a versatile tool for charged particle accelerator simulations", *J. Comput. Phys.*, vol. 229, no. 12, pp. 5020–5034, 2010. https://inspirehep.net/literature/1735290